JOURNAL OF MATERIALS SCIENCE 10 (1975) 593–598

Morphological changes occurring during reduction of WO_3

V. K. SARIN
Sandvik AB, Coromant Research Center, S-126 12 Stockholm 42, Sweden

The morphological changes occurring during the reduction of WO_3 seem to be quite unique. The initial reduction of WO_3 results in large plate-like whiskers of $WO_{2.72}$ of two morphologies, randomly oriented whiskers and clusters of whiskers. These decompose to form agglomerates of WO_2 (containing several small primary crystals), interlinked by chains of larger primary grains. The final reduction of WO_2 to tungsten is achieved without any further morphological change. From these observations it seems that formation of whiskers of $WO_{2.72}$ is the controlling step, in determining the final particle size of the tungsten powder.

1. Introduction

Tungsten forms a series of oxides with well-defined ordered phases, to which can be assigned precise stoichiometric formulae. These oxides have been extensively studied and are listed in Table I.

Preparation of tungsten powder is frequently undertaken by heating yellow tungstic oxide (WO_3) in a stream of hydrogen. In such a static bed, Millner [1] has suggested that the reduction reaction is controlled by the diffusion of water-vapour out of the boat containing the oxide. Parsons' [2] studies confirmed this and found that the reduction time was dependent on the powder bulk density, the bed temperature, and the diffusion path length. Practice supports these observations, since reduced oxides and metal powder are found as layers above the next higher oxide (for example W over WO_2 and WO_2 over $WO_{2.72}$, etc).

Several pertinent investigations, to list a few [1-5], have been conducted to explain the kinetics and thermodynamics of this reduction reaction. Although it is now fairly well understood, some conflicting results and controversies still exist. The study reported here was undertaken to observe the morphological changes occurring during the reduction of WO_3 through its series of oxides. Some investigations [6-8] have also been made on the TEM to try and follow the initial stages of this reduction reaction. But since there is still a relative dearth of information on this subject, it was felt that such information could further enhance existing knowledge regarding the kinetics of the reduction of WO_3.

2. Experimental procedure

Reduction of WO_3 was performed in a horizontal tube furnace using a static bed. High purity WO_3 (of the composition given in Table II) with an average particle size of 7.5 μm was used. For comparison purposes WO_3 powder with 0.02% Na was also investigated. A reduction temperature of 900° C and hydrogen with a dew point of around − 60° C was utilized in all cases. Powder

TABLE I Oxides of tungsten

Formula	Colour	Average at. ratio O/W	Structure	Density (g cm^{-3})
$WO_3(\alpha)$	yellow	3.00	Pseudorhombic. (R.T)*	7.29
$W_{20}O_{58}(\beta)$	blue-violet	2.90	Monoclinic	7.16
$W_{18}O_{49}(\gamma)$	reddish-violet	2.72	Monoclinic	7.78
$WO_2(\delta)$	brown	2.00	Monoclinic	10.82
$W_3O(\beta\text{-}W)$	grey	0.33	Cubic	11.4

*Has several different crystalline modifications depending on temperature.

© *1975 Chapman and Hall Ltd.*

TABLE II Nominal starting composition of WO_3 powder

Element	Sample A (wt %)	Sample B (wt %)
Fe	0.004	0.005
Si	< 0.002	< 0.002
Mo	0.07	0.07
As	< 0.002	< 0.002
Na	< 0.001	0.020
K	< 0.001	< 0.001
Ca	< 0.001	< 0.001
Av. grain size	7.5 μm	6.6 μm

was loosely packed (with an approximate packing density of 3.6 g cm^{-3} and a bed height of 1.8 cm) in rectangular boats and introduced into the furnace. By varying the reduction time, layer formation of all the oxides, in various stages of the reduction sequence were obtained. Samples were removed from the layers and then identified through X-ray examination and colour before being studied in the SEM.

Dynamic studies on some stages of this reduction process were also conducted in the TEM. WO_3 particles were suspended on tungsten grids and then reduced in a hydrogen atmosphere in the electron microscope. A thermogravimetric analysis of the reduction was also made.

3. Results and discussion

Since the basic aim of this study was to follow the reduction reaction through its various morphological changes, no attempt is made here to explain the thermodynamics of the process. The resultant oxides (Table I) could be easily identified by their distinctive colours, but X-ray diffraction was also utilized.

The sequence of the reduction of WO_3 to its lower oxides is still somewhat in a fluid state. In accordance with the layer formation obtained during this study, at 900° C, the following order can be predicted:

$$WO_3 \rightarrow \left\{\begin{matrix} W_{20}O_{58} \\ W_{18}O_{49} \end{matrix}\right\} \rightarrow WO_2 \rightarrow W$$

or

$$WO_3 \rightarrow \left\{\begin{matrix} WO_{2.90} \\ WO_{2.72} \end{matrix}\right\} \rightarrow WO_2 \rightarrow W\,.$$

It should be noted that $WO_{2.90}$ and $WO_{2.72}$ have been combined since the conversion of $WO_3 \rightarrow WO_{2.90} \rightarrow WO_{2.72}$ seems to be an extremely rapid reaction, hence only very small quantities of $WO_{2.90}$ were observed. Identification of $WO_{2.90}$ was only possible by its distinctive blue colour. These results were found to be in good agreement with the sequence of oxide formation obtained at 900° C under equilibrium conditions (Fig. 1).

The morphological changes occurring during the above mentioned sequence of oxide formation are shown in Figs. 2 to 7. As mentioned earlier, since very little $WO_{2.90}$ was obtained and since no morphological difference between $WO_{2.90}$ and $WO_{2.72}$ was observed in these samples, only $WO_{2.72}$ is considered here. The first step in the reduction of WO_3 to $WO_{2.72}$ consists of a transformation from well-defined crystals of WO_3 (Fig. 2) to plate-like whiskers of $WO_{2.72}$ (Figs. 3 and 4). As is evident, two types of such whiskers were observed, the randomly oriented (Fig. 3) and clusters (Fig. 4). The randomly oriented whiskers are believed to be formed from small WO_3 particles whereas the clusters are obtained from large WO_3 particles. The initial stages of such a cluster formation can be seen in Fig. 9, complete transformation of the WO_3 particle (black area) surrounded by the whiskers would yield a cluster. The length of these whiskers was found to vary anywhere from a few to 50 μm.

Transformation of $WO_{2.72}$ to WO_2 is obtained by the nucleation of small primary crystals at the centre of these clusters or by conversion of individual whiskers into single crystals of WO_2. The driving force of this process, besides the lowering of the oxygen potential, is obviously the reduction of the surface area to volume ratio, from platelets to crystalline form, which is energetically a more favourable morphology. Hence two different morphological structures of WO_2, large agglomerates containing several primary crystals and long chains of single crystals of WO_2 interlinking these grains, were obtained (Fig. 5). The individual crystals (in the chains) were generally found to be much larger than the primary crystals composing the large agglomerates (Fig. 6). The reduction of WO_2 to tungsten, apart from a reduction in particle size, was obtained without any further morphological change (Fig. 7).

A similar morphological sequence was observed to occur with Na doped WO_3 powder. The only difference observed was that the reduction rate was greatly enhanced, that is to say that Na effectively catalyses the reaction.

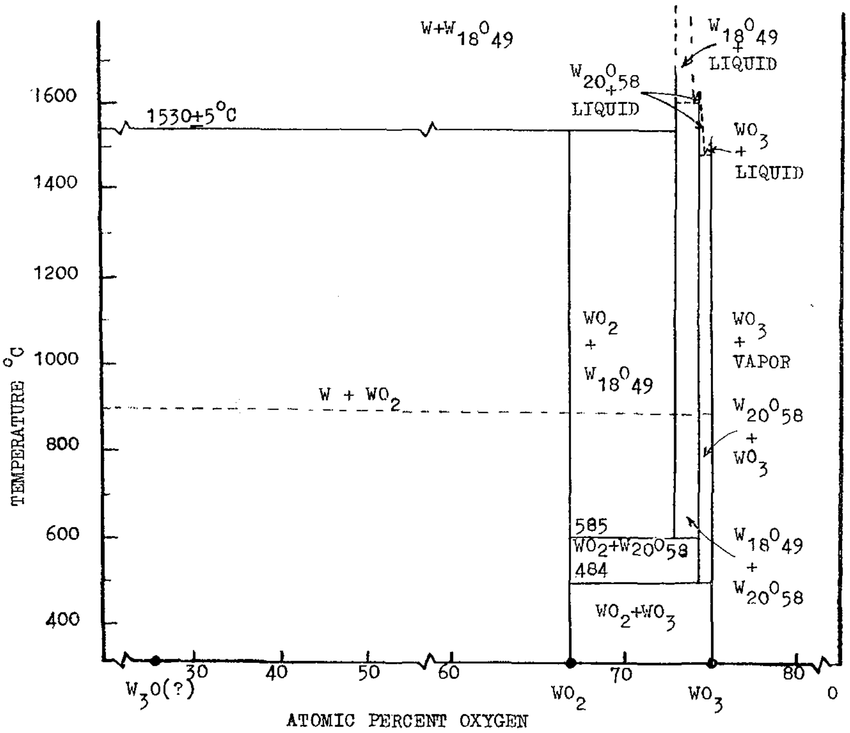

Figure 1 The system W–O as reported by Phillips [9]. Note that at 900°C with decreasing oxygen content the following sequence of oxide formation is obtained according to the above phase diagram:

$$\mathrm{WO_3} \rightarrow \begin{array}{c}\mathrm{W_{20}O_{58}}\\+\\\mathrm{WO_3}\end{array} \rightarrow \begin{array}{c}\mathrm{W_{18}O_{49}}\\+\\\mathrm{W_{20}O_{58}}\end{array} \rightarrow \begin{array}{c}\mathrm{WO_2}\\+\\\mathrm{W_{18}O_{49}}\end{array} \rightarrow \begin{array}{c}\mathrm{W}\\+\\\mathrm{WO_2}\end{array} \rightarrow \mathrm{W}\,.$$

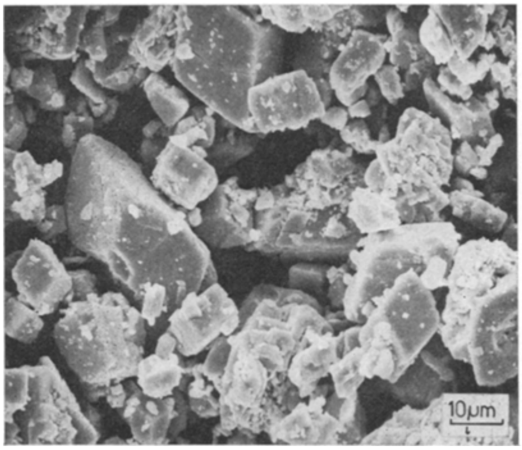

Figure 2 Typical structure of WO_3 powder.

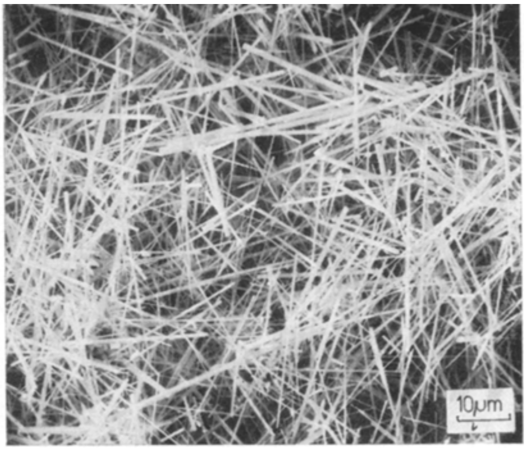

Figure 3 Random plate-like whiskers of $WO_{2.72}$ obtained upon initial thermal decomposition of WO_3.

Further study is needed to explain why eventually coarser tungsten powder is obtained with the addition of Na to WO_3 powder.

It has generally been reported that when pure WO_3 is reduced by hydrogen, large pseudo-crystals (agglomerates) containing several small (primary) crystals of tungsten are obtained. This

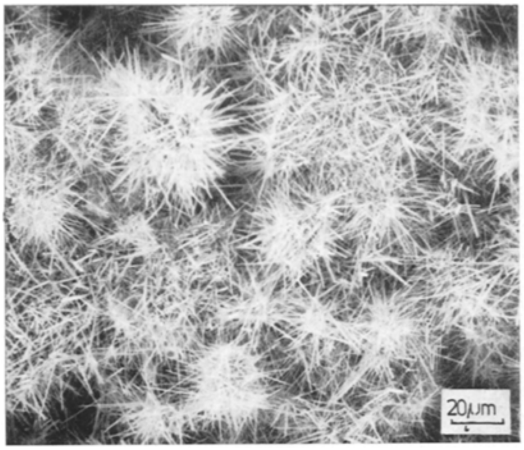

Figure 4 Clusters of $WO_{2.72}$ whiskers.

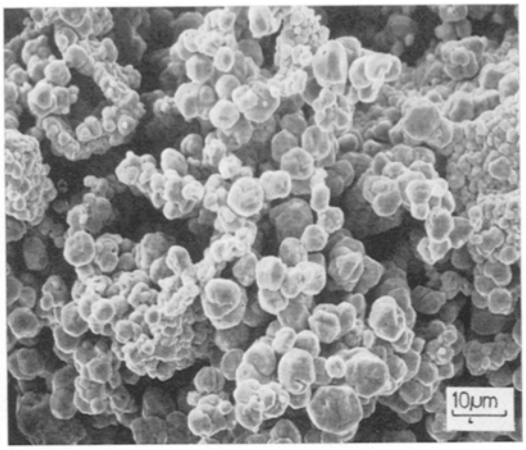

Figure 6 Typical structure of WO_2 (brown oxide).

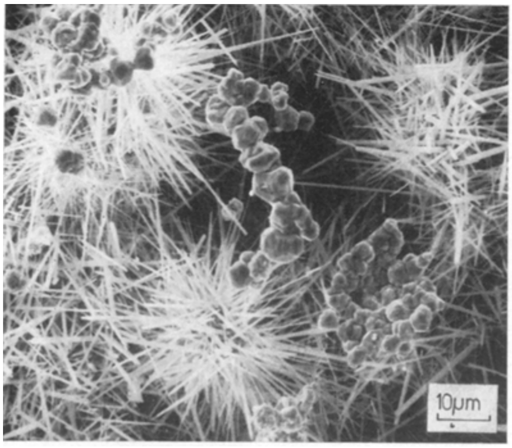

Figure 5 Conversion of whiskers of $WO_{2.72}$ to WO_2.

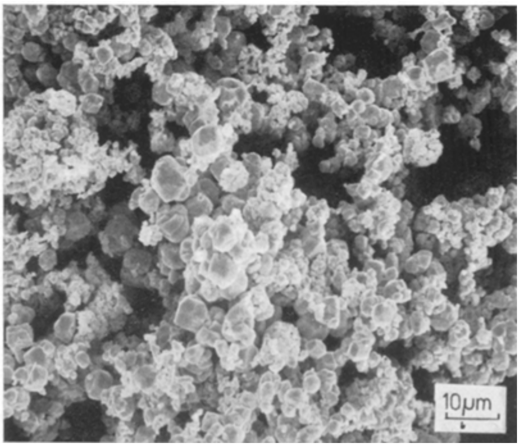

Figure 7 Structure of tungsten powder obtained on completion of the reduction reaction.

tungsten powder has been reported to maintain the size and shape of the original WO_3 powder. Hence the mechanism of this reaction has been associated with the original lattice being converted into tungsten via other lattices by solid-state reactions only [3]. Since the temperature range in which the reduction is normally carried out is 700 to 900°C, surface and self diffusion have been ruled out. On the other hand, when WO_3 is doped, the formation of a volatile tungsten compound $WO_2.nH_2O$ has been linked as the controlling factor in the reduction [3, 5, 10]. The compound $WO_3.H_2O$ has also been reported to be found on the passage of steam over pure WO_3 [11]. Results obtained in this study present the thesis that a volatile tungsten compound $WO_x.nH_2O$ (where $2 < x < 3$) is probably formed during the reduction of pure WO_3. The rapid formation of whiskers of $WO_{2.72}$, as large as 50 μm, seems to show evidence that probably a vapour to solid transformation is occurring.

It has been postulated that the presence of dope elements causes tungsten (in the α form, Table I) to be formed relatively early in the reduction process and the then volatile compound $WO_2.nH_2O$ decomposes in the neighbourhood of these tungsten "seeds" causing them to grow considerably [3]. The decomposition of this compound occurs according to the following equation [5]:

$$WO_2.nH_2O + 2H_2 \rightarrow W + (n + 2)H_2O$$

Considering the morphological sequence

obtained in this investigation it seems more likely that the volatile tungsten compound decomposes to form whiskers of $WO_{2.72}$. The decomposition could occur according to the following equation:

$$WO_x.nH_2O + (x - 2.72)H_2 \rightarrow WO_{2.72} + (x + n - 2.72)H_2O$$

From the morphological pattern observed, it appears that the final particle size of the tungsten powder formed is dependent on the size of the WO_2 particles which nucleate from the $WO_{2.72}$ whiskers. Therefore, the formation of whiskers of $WO_{2.72}$ and how WO_2 nucleates from them are probably the controlling steps in determining the final particle size of the tungsten powder. The effect of impurities (or dope elements) on the nucleation and growth of these whiskers and primary WO_2 particles, could result in the observed changes on the final particle size of the reduced tungsten powder.

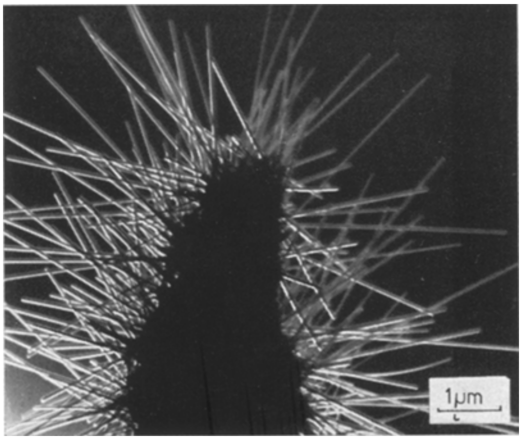

Figure 9 TEM photomicrograph showing initial formation of $WO_{2.72}$ whiskers.

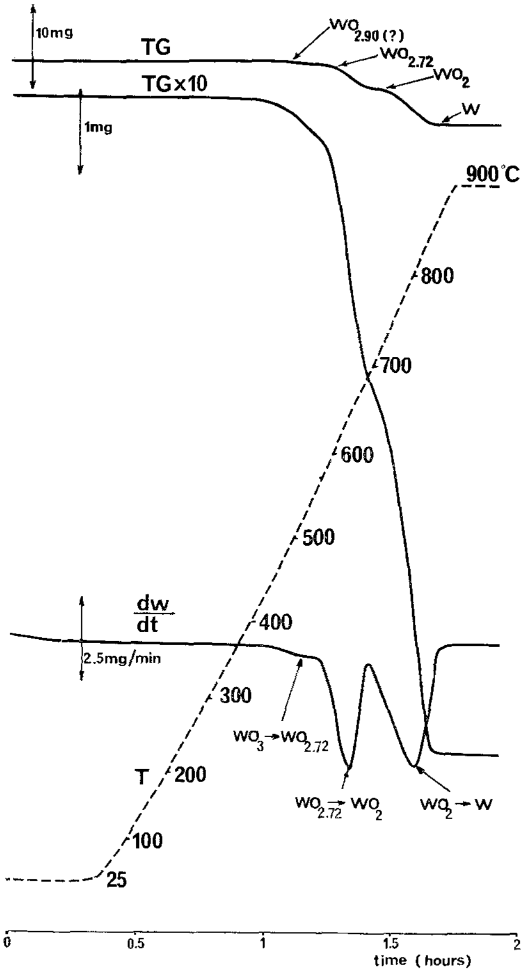

Figure 8 Thermogravimetric curve of the WO_3 reduction reaction.

Although the thermogravimetric analysis of the reduction reaction (Fig. 8) was not performed under identical conditions, the heating up time being much slower, a similar sequence of transformation was obtained.

Dynamic experiments, to continuously observe the initial stages of this reduction reaction were performed in the TEM. Fig. 9 shows whiskers of $WO_{2.72}$ formed by the initial thermal decomposition of WO_3. The whiskers were found to grow along the *b*-axis of the $WO_{2.72}$ monoclinic unit cell, with (010) as the growth plane (Fig. 10). Since the lattice of $WO_{2.72}$ is built up of WO_6 octahedra coupled together in an intricate way by sharing corners and edges [12], the fastest growth rate is probably achieved by the linking of these octahedra to form linear rows along the *b*-axis. The plate-like character of these whiskers is clearly evident from Fig. 11. Since the formation of these whiskers occurred at an extremely rapid rate, growth rates or their nucleation sites could not be determined. Upon further reduction, the whiskers were converted and formed particles of WO_2. These results confirmed the morphological sequence observed on the SEM.

4. Conclusions

The morphological changes occurring during the reduction of WO_3 seem to be quite unique, and have led to a new insight into this process. Owing to the formation of large whiskers of

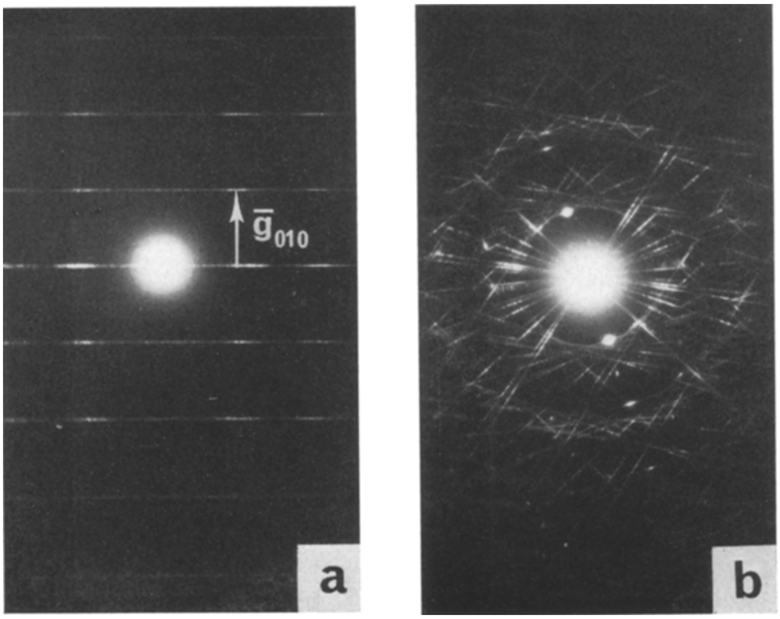

Figure 10 Diffraction pattern of $WO_{2.72}$ whiskers (a) obtained from several whiskers (b) from a single whisker.

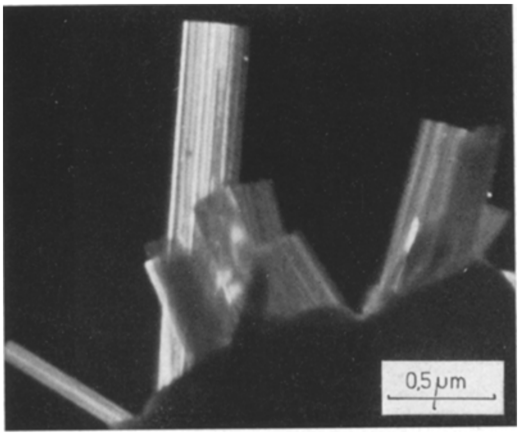

Figure 11 Dark-field image of a $WO_{2.72}$ whisker, showing its plate-like character (at 1000 kV).

$WO_{2.72}$ during initial stages of this reaction, a volatile compound $WO_x.nH_2O$ (where $2 < x < 3$) has been postulated. The decomposition of this compound results in plate-like whiskers of two morphologies, randomly oriented whiskers and clusters of whiskers. These result in agglomerates of WO_2 (containing several small primary crystals) interlinked by chains of larger primary crystals. The final reduction WO_2 to tungsten is achieved without any further morphological change. Preliminary investigations on the effect of Na on the reduction reaction have shown it to have no effect on the morphological sequence, although it catalyses the reaction.

Acknowledgements

The author is grateful to Sandvik AB for permission to publish this work. Stimulating discussions with members of the Coromant Research Center are greatly appreciated.

References

1. T. MILLNER, *Acta Tech.* **17** (1957) 67.
2. D. S. PARSONS, *Elect. Tech.* **3** (1965) 9.
3. H. L. SPIER, *Philips Res. Rep. Suppl.* **3** (1962) 52.
4. B. KOPELMAN, "The Physics of Powder Metallurgy", edited by W. Kingston (McGraw-Hill, New York, 1951) 303.
5. T. MILLNER, A. J. HEGEDÜS, K. SASVARI and J. NEUGEBAUER, *Z. Anorg. Chem.* **289** (1957) 288.
6. R. VEDA, *Nippon Kinzoku Gakkaishi* **23** (1959) 340.
7. *Idem, ibid* **23** (1959) 422.
8. H. HASHIMOTO, T. NAIKI, T. ETA and K. FUJIWARA, *Jap. J. Appl. Phys.* **7** (1968) 946.
9. B. PHILLIPS and L. L. Y. CHANG, *Trans. Met. Soc. AIME* **230** (1964) 1203.
10. B. KOPELMAN, AIME Tech. Publ. 2100 (1946) 1.
11. G. MEIJER, J. F. OOSTROM and W. J. VAN OEVÉRÉN, *Rec. Trav. Chim. Pays-Bas* **78** (1959) 417.
12. A. MAGNÉLI, *Arkiv Kemi* **1** (1949) 223.

Received 16 September and accepted 7 October 1974.